Green Chemistry

Accepted Manuscript

ROYAL SOCIETY OF CHEMISTRY

www.rsc.org/greenchem

Cite this: DOI: 10.1039/c0xx00000x

www.rsc.org/xxxxxx

ARTICLE TYPE

Towards sustainable synthesis of pyren-1-yl azoliums via electrochemical oxidative C–N coupling†

Guillaume de Robillard,[a] Oumayma Makni,[a] Hélène Cattey,[a] Jacques Andrieu[a]* and Charles H. Devillers[a]*

Received (in XXX, XXX) Xth XXXXXXXXX 20XX, Accepted Xth XXXXXXXXX 20XX
DOI: 10.1039/b000000x

Electrosynthesis of 1-methyl-3-(pyren-1-yl)-1*H*-imidazol-3-ium tetrafluoroborate via oxidative C-N coupling of pyrene with methylimidazole is optimized with the aim to reduce waste and simplify the experimental setup. Several parameters are tested such as cell configuration (number of compartments), pyrene concentration, amount of nucleophile, electrosynthetic method (potentiostatic/galvanostatic), amount of electrons, atmosphere (Ar/air), solvent quality and presence/absence of supporting electrolyte. The optimized conditions are successfully applied to the synthesis of 1-methyl-3-(pyren-1-yl)-1*H*-benzimidazol-3-ium tetrafluoroborate, 1-methyl-4-(pyren-1-yl)-1*H*-1,2,4-triazol-4-ium tetrafluoroborate and 3-(pyren-1-yl)-benzothiazol-3-ium tetrafluoroborate. These four pyren-1yl-azolium salts are characterized by NMR, MS, elemental analysis, UV-Vis. absorption and emission spectroscopies. The X-ray crystallographic structures of 1-methyl-3-(pyren-1-yl)-1*H*-imidazol-3-ium tetrafluoroborate and 1-methyl-3-(pyren-1-yl)-1*H*-benzimidazol-3-ium tetrafluoroborate are presented.

Introduction

Pyrene is probably one of the most employed and studied organic chromophore. This aromatic compound has attracted considerable attention since its discovery in 1837 by Laurent[1] due to its unique photochemical and photophysical properties.[2] Pyrene is used as a fluorescent label in many studies such as determination of peptide and protein structures,[3] interactions of molecules with DNA/RNA.[4] In certain conditions, pyrene π-dimers are formed by inter-[5] and/or intramolecular[6] π-π interactions. These assemblies, called excimers, are exploited for (bio)sensor applications[7] and host-guest detection[8] since the change of the excimer fluorescence intensity and wavelength is sensitive to the pyrene microenvironment.[9] This aromatic dye strongly interacts with carbon materials such as highly oriented pyrolytic graphite (HOPG),[10] graphene/reduced graphene oxide,[11,12] and carbon nanotubes[7,13] via π-π stacking interactions. This interesting property leads to applications in catalysis allowing the catalyst to be recycled numerous times.[12] Pyrene-based materials have also been produced by electropolymerization of pyrene,[14,15] polymerization of a suitable polymerizable moiety covalently linked to pyrene[16] or electropolymerization of pyrene-based copolymers.[17] These materials find applications in organic electronics such as organic photovoltaic cells,[18] organic light-emitting diodes,[19] organic field-effect transistors[20] and organic lasers.[21]

All these tremendous physico-chemical properties initially lie on the remarkable progresses achieved on pyrene functionalization. Nowadays, all pyrene positions can be substituted. Thus, 1-substituted[22] and 1,3,6,8-substituted pyrenes are easily available by direct electrophilic substitution of pyrene[23] whereas the 1,6- and 1,8-disubstituted isomers are still much harder to synthesize selectively. The 1,3-disubstituted derivative is generally obtained as a minor fraction from the synthesis of 1,6- and 1,8-disubstitued pyrenes but a new selective route for the preparation of this compound was reported seven years ago.[24] Recently, the direct functionalization of pyrene in 2,7-positions by boronate esters was achieved using an iridium catalyst.[25] The 4,5,9,10 positions have been substituted using a mixture of $RuCl_3$ and $NaIO_4$[26] or by bromination of a "protected" 2,7-di-*tert*-butylpyrene.[27] These chemical syntheses generally require either toxic/dangerous reactants (Br_2, HNO_3...) or expensive metals (Ir, Ru). Given the redox properties of pyrene, *i.e.* this latter can be oxidized or reduced, another alternative route for its functionalization consists in its electrochemical transformation. Surprisingly, this route has only been sparingly explored. Thus, *tert*-butylation[28] and isopropylation[29] have been performed by electrochemical reduction of pyrene in presence of the corresponding alkyl chlorides. However, yields were rather modest especially for isopropyl-substituted pyrene because numerous isomers and dehydrogenated compounds were produced. By contrast, anodic nucleophilic substitution of pyrene with pyridine and 1-methylimidazole (**MeIm**) provides the resulting $C_{(pyrene)}$-$N_{(Nucleophile)}$ linked pyren-1-yl pyridinium and 1-pyren-1-yl imidazolium perchlorate salts in very good yields and perfect regioselectivity.[30] This reaction constitutes a rare example of pyrene direct C-H activation. Very recently, the electrochemical aromatic C-H/imidazole coupling has been reported by Yoshida and co-workers with phenyl-based compounds, naphthalene and phenanthrene.[31] It should be stressed that the formation of C-N bonds is a highly competitive

field since numerous pharmaceutical targets contain imidazole-based compounds with this C-N linkage.[31] Common synthetic routes leading to nitrogen-substituted aromatic compounds consist in the chemical transformation of amino aromatic derivatives[32] or the transition metal-catalyzed C−N (amine or amide) bond formation from halo-aryl precursors.[33] However, transition-metal catalysts become more and more expensive due to tedious extraction and purification procedures and increasing demand in electronic applications.

Recently, our group was interested in the synthesis of neutral carbenes by electroreduction of their corresponding imidazolium salts. We showed that CO_2 could be trapped by the *in situ* formed carbenes providing the imidazolium carboxylate zwitterions.[34] These masked carbenes can react with numerous transition metals[35,36] and electrophiles[35,37] and are also useful building blocks to generate halide-free ionic liquids or imidazolium salts.[38] 1-methylimidazolium pyrene is a very interesting candidate for the production of an original carbene since the pyrene moiety could bring additional physico-chemical properties such as fluorescence, immobilization on carbon materials or electropolymerization. Having already experienced the anodic nucleophilic substitution method,[39] we wanted to synthesize this product reproducing first the conditions of Iyoda and co-workers.[30] Thus, this manuscript deals with the optimization of the experimental conditions previously described,[30] applied to the synthesis of 1-methyl-3-(pyren-1-yl)-1*H*-imidazol-3-ium tetrafluoroborate salt, $\mathbf{1^+,BF_4^-}$ (Fig. 1).

Our main goal is to decrease cost and environmental impact of this anodic nucleophilic substitution. Furthermore, to extend the scope of this valuable reaction, other azole nucleophiles, *i.e.* methylbenzimidazole (**MeBzIm**), 1-methyl-2,4-triazole (**MeTrz**) and benzothiazole (**BzThz**) have been tested and successful functionalization of the pyrene on the 1-position was performed leading to unprecedented 1-methyl-3-(pyren-1-yl)-1*H*-benzimidazol-3-ium tetrafluoroborate ($\mathbf{2^+,BF_4^-}$), 1-methyl-4-(pyren-1-yl)-1*H*-1,2,4-triazol-4-ium tetrafluoroborate ($\mathbf{3^+,BF_4^-}$) and 3-(pyren-1-yl)-benzothiazol-3-ium tetrafluoroborate ($\mathbf{4^+,BF_4^-}$) targets (Fig. 1).

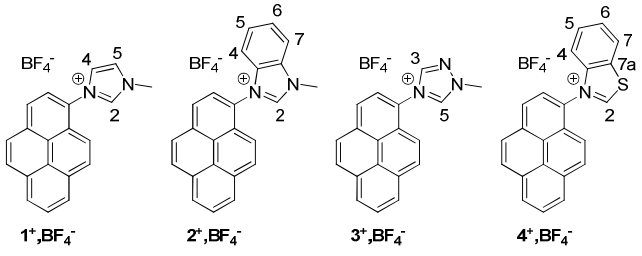

Fig. 1 Structures of the electrosynthesized pyren-1-yl azoliums. Some atoms are labelled according to NMR data (see experimental section).

Results and discussions

Optimization of the experimental conditions for the synthesis of 1-methylimidazoliumpyrene ($\mathbf{1^+,BF_4^-}$)

All potential values in this manuscript will be given *vs.* the saturated KCl calomel reference electrode (SCE) unless otherwise noted.

The synthetic conditions previously reported by Iyoda and co-workers for the formation of 1-methylimidazoliumpyrene perchlorate ($\mathbf{1^+,ClO_4^-}$) consist in a potentiostatic electrolysis in a standard three electrode cell (in a three compartment configuration, *i.e.* each electrode is separated from the others by a sintered glass disk), at a potential corresponding to the first oxidation of pyrene (1.20 V *vs.* Ag/Ag^+, *i.e.* 1.44 V *vs.* SCE) in presence of 50 mM pyrene in CH_3CN 0.5 M $NaClO_4$ and 10 molar equivalents of **MeIm** (entry 1, Table 1).[30]

Our first optimizations involve the replacement of the sodium perchlorate supporting electrolyte by tetraethylammonium tetrafluoroborate ($TEABF_4$) at lower concentration (from 0.5 M to 0.1 M). This supporting electrolyte is chosen since it exhibits good solubility in acetonitrile and water, is less hygroscopic and safer to handle than sodium perchlorate. Alternative polar aprotic solvents to acetonitrile could have been dimethylformamide, dimethylacetamide or *N*-methylpyrrolidinone but these latter are classified as "undesirable" solvents[40] due to their toxicity (classified as "substances of very high concern" in the EU since they are toxic for reproduction).[41] Moreover, dimethylformamide is classified as a hazardous airborne pollutant in the US[40]. Acetonitrile was finally kept since this solvent is considered as a "usable" solvent[40] and it allows to work with very high positive potentials.

Besides, the amount of **MeIm** was initially reduced from 10 to 6 molar equivalents *vs.* pyrene. Another improvement consists in the addition of a small amount of HBF_4 (1.5 eq. *vs.* pyrene) which allows working with only two compartments, *i.e.* the anode and the cathode reside in the same compartment. This acid is chosen since its anion is the same as the supporting electrolyte. Moreover, this cell setup is preferred for industrial applications since the use of glass frits/membranes between these two electrodes is thus avoided. Oxidation of pyrene at the anode and reduction of protons at the cathode are thus the expected reactions.

The cyclic voltammogram of pyrene in CH_3CN 0.1 M $TEABF_4$ exhibits two irreversible oxidation processes at E_{pa} = 1.40 V and E_{pa} = 1.91 V (cation radical and dication formation, respectively) and one monoelectronic reversible reduction, at $E_{1/2}$ = −2.12 V (anion radical formation), as already reported[14] (Fig. 2, top, black solid curve).

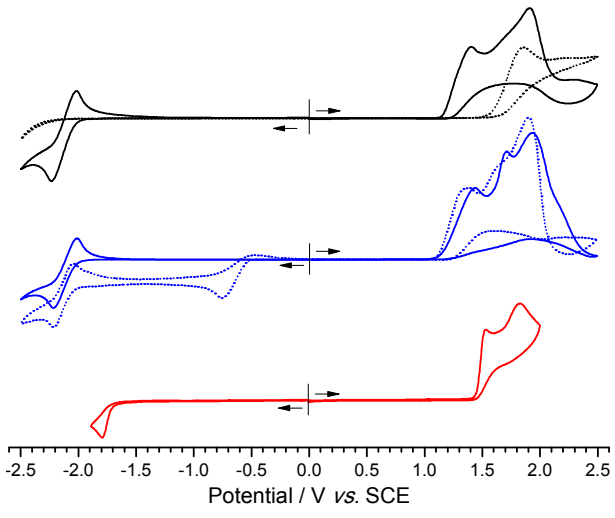

Fig. 2 Cyclic voltammograms of pyrene (top, black solid line), MeIm (top, black dotted line), pyrene + 6 eq. MeIm (middle, blue solid line), pyrene + 6 eq. MeIm + 1.5 eq. HBF_4 (middle, blue dotted line), **1**$^+$,BF_4^- (bottom, red solid line) in CH_3CN 0.1 M $TEABF_4$ (WE: Pt Ø = 2 mm, v = 100 mV s^{-1}).

After addition of 6 equivalents of **MeIm** to the pyrene solution, the cyclic voltammogram shows a new oxidation peak at E_{pa} = 1.71 V (Fig. 2, middle, blue solid curve).This redox system does not correspond to the direct oxidation of **MeIm** since this latter is irreversibly oxidized at higher potential (E_{pa} = 1.85 V (Fig. 2, top, black dotted curve)). After addition of 1.5 equivalents of HBF_4, 1.5 equivalents of **MeIm** are protonated (**MeIm-H**$^+$,BF_4^-). Irreversible reduction of this species is clearly seen at E_{pc} = −0.76 V (Fig. 2, middle, blue dotted curve). Thus, **MeIm-H**$^+$,BF_4^- is the first reactant to be reduced, leading to **MeIm** and H_2. Consequently, in a single compartment electrochemical cell, oxidation of pyrene will happen at the anode while reduction of **MeIm-H**$^+$,BF_4^- will proceed at the cathode. Theoretically, the anodic nucleophilic substitution reaction requires abstraction of 2 molar equivalents of electrons from pyrene.[31,42] This reaction starts with the formation of pyrene cation radical (**Pyr**$^{\bullet+}$,BF_4^-, Scheme 1) which is then attacked by **MeIm** nucleophile. This cationic intermediate (**Pyr-MeIm**$^{\bullet+}$, BF_4^-, Scheme 1) is oxidized and releases one proton providing **1**$^+$,BF_4^-. In return, the cathodic reaction must involve 2 F and thus two equivalents of **MeIm-H**$^+$,BF_4^- must be reduced at the cathode. As only one molar equivalent of protons is generated during the formation of **1**$^+$,BF_4^-, initial addition of at least one equivalent of H^+ is needed to preclude other reactions than reduction of protons to happen at the cathode.

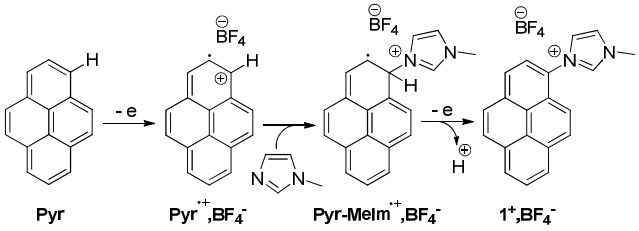

Scheme 1 Proposed reaction mechanism for the electrochemical formation of **1**$^+$,BF_4^-.

Bulk electrolyses were first performed with 6 equivalents of **MeIm** (entry 2, Table 1) in a three electrodes/two compartments configuration under potentiostatic conditions (E_{app} = 1.40 V). 3.25 Faradays (F) were necessary for full conversion of pyrene. In these conditions a yield as high as 92% was obtained denoting the perfect regioselectivity of this anodic nucleophilic substitution. It should be noted that no other pyrene-based product was detected on the ^{1}H NMR spectrum of the crude solution. Besides, the cyclic voltammogram of the electrolyzed crude solution do not show any trace corresponding to the initial unsubstituted pyrene oxidation confirming that this species was fully exhausted. Furthermore, new irreversible oxidation (E_{pa} = 1.54 V) and reduction (E_{pc} = −1.79 V) peaks which corresponds to the oxidation and reduction of the electrogenerated **1**$^+$,BF_4^- are clearly seen at the end of the electrolysis (see Fig. 2, bottom, red curve, for the cyclic voltammogram of pure **1**$^+$,BF_4^-). The peak located at E_{pc} = −1.79 V reasonably corresponds to the reduction of the imidazolium moiety of **1**$^+$,BF_4^- since this potential value falls within the common potential range found for the reduction of imidazolium compounds.[43]

Decreasing the amount of **MeIm** from 6 to 3 equivalents does not change the yield of the reaction and only 2.35 Faradays were required (entry 3, Table 1). Under these conditions, but at lower concentration ([pyrene] = 4.8×10^{-4} M, Fig. 3), the UV-vis. spectrum of the reacting solution has been monitored as a function of the electrolysis progress. The initial pyrene signature with band maxima at λ = 262, 273, 305, 319 and 334 nm is progressively substituted by a new bathochromically shifted spectrum appearing at λ = 265, 275, 314, 326 and 341 nm which corresponds to **1**$^+$,BF_4^-. The presence of 7 isosbestic points at λ = 263, 268, 309, 313, 322, 330 and 337 nm confirms the simple transformation of the initial pyrene into **1**$^+$,BF_4^-, with no intermediate observed between.

Following the conditions of entry 3, the electrosynthesis was attempted with undistilled CH_3CN and under air (entry 4, Table 1). These conditions have been tested since they are easy to implement and they could be easily scaled up for industrial applications. Moreover, it is expected that **MeIm-H**$^+$,BF_4^- will be reduced at a higher potential than oxygen and thus this latter will not interfere. Besides, production of potentially recoverable hydrogen gas during the electrosynthesis will progressively drive away the initial air atmosphere. Though full conversion of the initial pyrene reactant was not reached and number of abstracted electrons was higher than theoretically expected (3.25 F), the yield remained very good (84%).

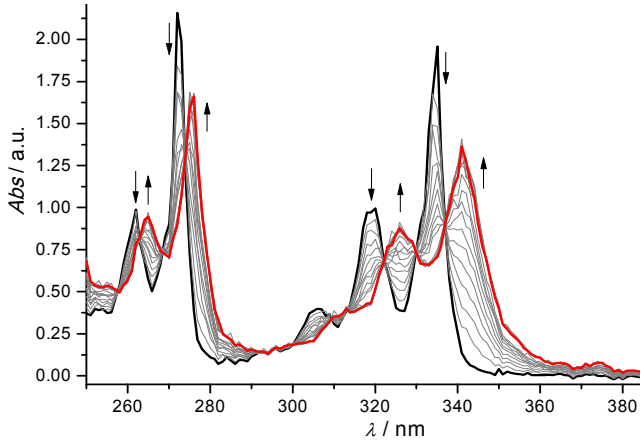

Fig. 3 Electrolysis of a 4.8×10^{-4} M solution of pyrene with 3 equiv. of 1-MeIm and 1.5 equiv. of HBF_4 followed by UV-vis spectroscopy (l = 2 mm, 0.1 M $TEABF_4$ in CH_3CN, E_{app} = 1.40 V *vs.* SCE, −2.20 F, WE: Pt wire, WE and counter-electrode are in the same compartment).

An experiment with only 2 equiv. of **MeIm** and 1 equiv. of tetrafluoroboric acid was attempted but full conversion of the pyrene was not possible even after reaching the theoretical value of 2 F (entry 5, Table 1). Nevertheless, a correct yield of 75% was obtained.

An upscale of the reaction was tested in the same conditions as entry 3 (entry 6, Table 1) but on 3.500 g of pyrene at higher concentration. After abstraction of only 2.05 molar equivalents of electrons, very close to the theoretical value of 2 F, a 95% yield was reached denoting the even higher efficiency of this electrosynthesis on larger scale.

For industrial applications, the cell setup must be as simple and as cheap as possible. Thus, a one compartment cell containing

only two electrodes (anode and cathode) and galvanostatic conditions are generally preferred. Besides, in order to decrease the waste and the price of the reaction, the amount of solvent must be as low as possible. That is why conditions of entry 7, where the major part of pyrene is not solubilized (solution saturation is reached at *ca*. 0.1 M) have been tested. A constant current of 50 mA was applied until 2.05 F has been passed. In these unconventional conditions, 92% of pyrene is consumed and a 94% yield was reached based on this conversion.

Table 1 Tested conditions for the synthesis of $\mathbf{1}^+,\mathbf{BF_4}^-$ (entries 2-8) and experimental conditions used for the synthesis of $\mathbf{2}^+,\mathbf{BF_4}^-$, $\mathbf{3}^+,\mathbf{BF_4}^-$ and $\mathbf{4}^+,\mathbf{BF_4}^-$ (entries 9-11), see ESI for experimental details.[a]

Entry	# of compartments / # of electrodes	m_{pyrene} (g) / *[pyrene]* (mM)	Nucleophile / equiv. *vs*. pyrene	Equiv. HBF_4 *vs*. pyrene	E_{app} (V/SCE) / i_{app} (mA)	conversion (%)[b]	*Faraday vs*. pyrene	Atom efficiency (%)[c]	E_m (E_M) factors[c]	Yield (%)[d]
1 (ref. 30)[e]	3 / 3	0.506 / 48	MeIm / 10	0	1.44 V	–	2.20	30	2.68 (2.27)	90
2	2 / 3	0.253 / 41	MeIm / 6	1.5	1.40 V	100	3.25	45	1.44 (1.23)	92
3	2 / 3	0.253 / 41	MeIm / 3	1.5	1.40 V	100	2.35	64	0.71 (0.57)	92
4[f]	2 / 3	0.253 / 41	MeIm / 3	1.5	1.40 V	93	3.25	64	0.71 (0.57)	84 (90[i])
5	2 / 3	0.253 / 41	MeIm / 2	1	1.40 V	82	2.00	81	0.65 (0.23)	75 (91[i])
6	2 / 3	3.500 / 100	MeIm / 3	1.5	1.40 V	100	2.05	64	0.65 (0.57)	95
7	1 / 2	4.045 / 692[g]	MeIm / 3	1.5	50 mA	92[h]	2.05	64	0.82 (0.57)	86 (94[i])
8[j]	1 / 2	4.045 / 692[g]	MeIm / 3	1.5	50 mA	87[h]	2.05	64	0.96 (0.57)	80 (92[i])
9	2 / 3	0.253 / 41	MeBzIm / 3	1.5	1.40 V	100	2.66	58	1.13 (0.74)	82
10	2 / 3	0.253 / 41	MeTrz / 3	1.5	1.40 V	100	2.55	64	1.05 (0.57)	88
11	2 / 3	0.253 / 41	BzThz / 3	1.5	1.40 V	100	3.00	57	2.04 (0.75)	57

[a] Conditions common to all experiments (excepted otherwise noted): room temperature, under Ar, CH_3CN 0.1 M $TEABF_4$, Pt for anode and cathode. [b] Estimated with the ratio $((i_{initial} - i_{final}) / i_{initial}) \times 100)$ measured by cyclic voltammetry on the first oxidation peak of the pyrene. [c] See definitions and calculations in ESI (S20). [d] Obtained for isolated compounds. [e] Work performed with 0.5 M $NaClO_4$. [f] Under air atmosphere, with undistilled CH_3CN. [g] Theoretical concentration since pyrene is not fully soluble at this concentration. [h] Calculated from the remaining amount of isolated pyrene. [i] Isolated yield calculated considering the "conversion" column. [j] Without $TEABF_4$ supporting electrolyte.

In conditions of entry 7, the amount of HBF_4 (in its **MeIm-H$^+$,BF$_4^-$** form) is higher than 0.5 eq. *vs*. pyrene up to the end of the electrolysis, *i.e*. its concentration is higher than 0.34 M (for abstraction of 2 F). Thus, it could be potentially used as a supporting electrolyte. Indeed, supporting electrolyte such as $TEABF_4$ can be an important source of waste. Consequently conditions of entry 8, similar to entry 7 but without $TEABF_4$ have been tested. In these conditions, 87% of pyrene is consumed and a 92% yield was reached based on this conversion.

In order to evaluate the environmental benefits of our optimized synthesis, atom efficiency,[44] E_m and E_M factors[45] have been calculated for all entries of Table 1 (see example of calculations in ESI, S19). Considering the atom efficiency, all experimental conditions reported in Table 1 give higher values than reported before by Iyoda and co-workers[30] (30%, entry 1, Table 1) since the amount of nucleophile has been reduced. The best atom efficiency value (81%) is reached for conditions of entry 5 for which only 2 equivalents of nucleophile are used but this result must be balanced by the lower synthetic yield obtained. The E_m and E_M factors have also been compared with entry 1. E_m is significantly improved since its value is divided up to a factor of 4.1 (from 2.68, entry 1 to 0.65, entry 5-6) whereas E_M is greatly reduced from 2.27 to 0.23, *i.e*. a 9.9 decrease factor (entry 1 *vs*. entry 5). These improved parameters are in agreement with a greener and more sustainable process for our electrosynthetic conditions.

Having these optimized conditions in hand, we wanted next to extend the scope of this efficient electrochemical reaction to different kinds of azole nucleophiles.

Electrosynthesis of azolium compounds

Azolium salts are very useful compounds since their deprotonation leads to carbenes which are exploited as simple building blocks,[46] or in various reactions such as organocatalysis[47] and organometallic catalysis.[48] We have tested different kinds of azole nucleophiles, *i.e*. 1-methylbenzimidazole (**MeBzIm**), 1-methyl-2,4-triazole (**MeTrz**) and benzothiazole (**BzThz**). These nucleophiles have been selected since they are oxidized at higher potential than pyrene (E_{pa} = 1.80, 1.80, >2.5 and 2.32 V for **MeIm**, **MeBzIm**, **MeTrz** and **BzThz**, respectively) and they have been already used as precursors of azolium salts.[46,47,48] Keeping one of the best conditions for the synthesis of $\mathbf{1}^+,\mathbf{BF_4}^-$ (entry 3, Table 1), the unreported 1-methylbenzimidazoliumpyrene ($\mathbf{2}^+,\mathbf{BF_4}^-$), 1-(1-methyl-2,4-triazolium)pyrene ($\mathbf{3}^+,\mathbf{BF_4}^-$) and 1-benzothiazoliumpyrene ($\mathbf{4}^+,\mathbf{BF_4}^-$) are produced in 82, 88 and 57% yield, respectively (entry 10-12, Table 1). The relatively modest yield obtained for $\mathbf{4}^+,\mathbf{BF_4}^-$ is not due to the formation of unwanted side-products during the electrolysis but arises from difficulties to isolate the product in a pure form.

The ^{1}H NMR spectra of the pyren-1-yl azoliums exhibit characteristic low field signals (from 8.8 to 7.5 ppm) attributed to the pyrene core. The singlet corresponding to the procarbenic proton(s) appears at 9.74 ppm (H2, see attribution on Fig. 1, $\mathbf{1}^+,\mathbf{BF_4}^-$, DMSO-d6), 10.02 ppm (H2, $\mathbf{2}^+,\mathbf{BF_4}^-$, acetone-d6), 10.75 and 9.79 ppm (H5 and H3, $\mathbf{3}^+,\mathbf{BF_4}^-$, DMSO-d6) and 11.13 ppm (H2, $\mathbf{4}^+,\mathbf{BF_4}^-$, acetone-d6). The carbon atom(s) linked to this(these) proton(s) also exhibit(s) a low field signal at 138.7 ppm (C2, see attribution on Fig.1, $\mathbf{1}^+,\mathbf{BF_4}^-$), 145.0 ppm (C2, $\mathbf{2}^+,\mathbf{BF_4}^-$), 145.5 and 144.5 ppm (C5 and C3, $\mathbf{3}^+,\mathbf{BF_4}^-$) and 143.9 ppm (C2, $\mathbf{4}^+,\mathbf{BF_4}^-$).

The UV-visible spectra of these azolium salts in CH_3CN exhibit well resolved bands which are very similar in terms of maxima and molar extinction coefficients (Fig. 4). Substitution of the pyrene with one azolium fragment causes a slight bathochromic shift (*ca*. 7 nm).

By contrast, the emission spectra of $\mathbf{1}^+,\mathbf{BF_4}^-$, $\mathbf{2}^+,\mathbf{BF_4}^-$, $\mathbf{3}^+,\mathbf{BF_4}^-$ and $\mathbf{4}^+,\mathbf{BF_4}^-$ are very different (Fig. 5). Indeed, whereas $\mathbf{1}^+,\mathbf{BF_4}^-$ exhibits only monomeric emission at the studied concentration (*C*

= 1.25×10^{-5} M) and is highly fluorescent (see ESI, S17, Table S1 for comparative emission intensities), $\mathbf{2}^{+},\mathbf{BF_4}^{-}$, $\mathbf{3}^{+},\mathbf{BF_4}^{-}$ and $\mathbf{4}^{+},\mathbf{BF_4}^{-}$ show an important contribution of the featureless excimer emission, especially for $\mathbf{2}^{+},\mathbf{BF_4}^{-}$ (see ESI, S17, Fig. S13), and lower emission intensities. In particular, the emission of $\mathbf{2}^{+},\mathbf{BF_4}^{-}$ and $\mathbf{4}^{+},\mathbf{BF_4}^{-}$, the sole compounds bearing a phenyl fragment fused to the azolium moiety, is almost fully quenched (Fig. 5). Interestingly, contrary to $\mathbf{4}^{+},\mathbf{BF_4}^{-}$, $\mathbf{1}^{+},\mathbf{BF_4}^{-}$, $\mathbf{2}^{+},\mathbf{BF_4}^{-}$ and $\mathbf{3}^{+},\mathbf{BF_4}^{-}$ are fluorescent in the solid state (see ESI, S17, Fig. S14 for pictures of the solids under UV irradiation).

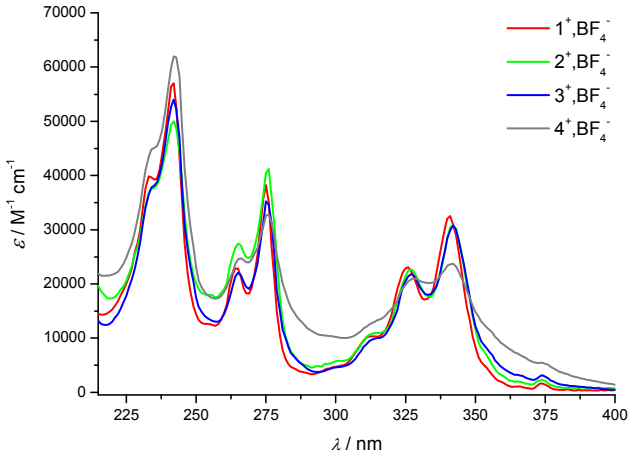

Fig. 4 UV-vis. absorption spectra of $\mathbf{1}^{+},\mathbf{BF_4}^{-}$, $\mathbf{2}^{+},\mathbf{BF_4}^{-}$, $\mathbf{3}^{+},\mathbf{BF_4}^{-}$ and $\mathbf{4}^{+},\mathbf{BF_4}^{-}$ in CH_3CN.

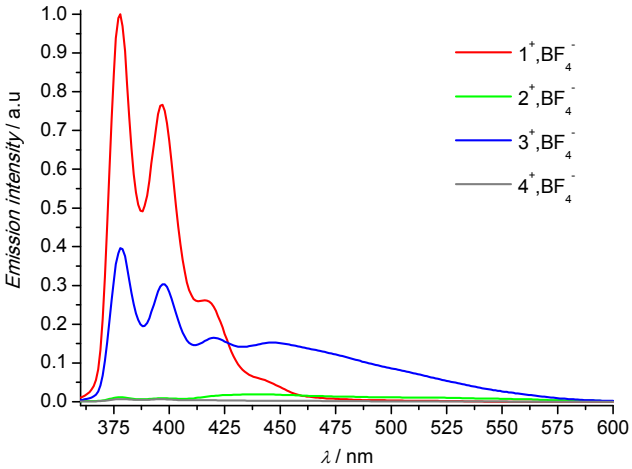

Fig. 5. Emission spectra of $\mathbf{1}^{+},\mathbf{BF_4}^{-}$, $\mathbf{2}^{+},\mathbf{BF_4}^{-}$, $\mathbf{3}^{+},\mathbf{BF_4}^{-}$ and $\mathbf{4}^{+},\mathbf{BF_4}^{-}$ in CH_3CN (identical measurement parameters for each compound, C = 1.25×10^{-5} M, $\lambda_{excitation}$ = 341 nm).

Crystallography

Crystallographic structures of $\mathbf{1}^{+},\mathbf{BF_4}^{-}$ and $\mathbf{2}^{+},\mathbf{BF_4}^{-}$ were investigated in the course of this work. Suitable crystals for X-ray diffraction studies were obtained by recrystallization of a CH_3CN/THF solution of $\mathbf{1}^{+},\mathbf{BF_4}^{-}$ and slow evaporation of a CH_3CN solution of $\mathbf{2}^{+},\mathbf{BF_4}^{-}$. Three-dimensional molecular views are presented in Fig. 6 and Fig. 7. The dihedral angle between the imidazolium moieties and the pyrene least square plane is equal to 73.10(4)° for $\mathbf{1}^{+},\mathbf{BF_4}^{-}$ and 77.40(2) for $\mathbf{2}^{+},\mathbf{BF_4}^{-}$. The C_{pyrene}-$N_{imidazolium}$ distances are similar: N1-C5 = 1.443(2) Å and C9-N1 = 1.4458(17) Å for $\mathbf{1}^{+},\mathbf{BF_4}^{-}$ and $\mathbf{2}^{+},\mathbf{BF_4}^{-}$, respectively. The unit cell of $\mathbf{1}^{+},\mathbf{BF_4}^{-}$ contains four groups of dimers differently oriented. Each dimer is composed by two parallel head-to-tail π-stacked pyrene groups contrary to what is reported for 1-bromopyrene where the bromide atoms are oriented towards the same direction.[49] The interplanar and the centroid to centroid (calculated from the 16 pyrene carbon atoms) distances for the dimer are 3.4498(9) Å and 3.9206(9) Å, respectively, leading to a slippage distance equal to 1.8628(12) Å. $\mathbf{2}^{+},\mathbf{BF_4}^{-}$ also forms dimers, which are all parallel and assembled in a head-to-tail π-

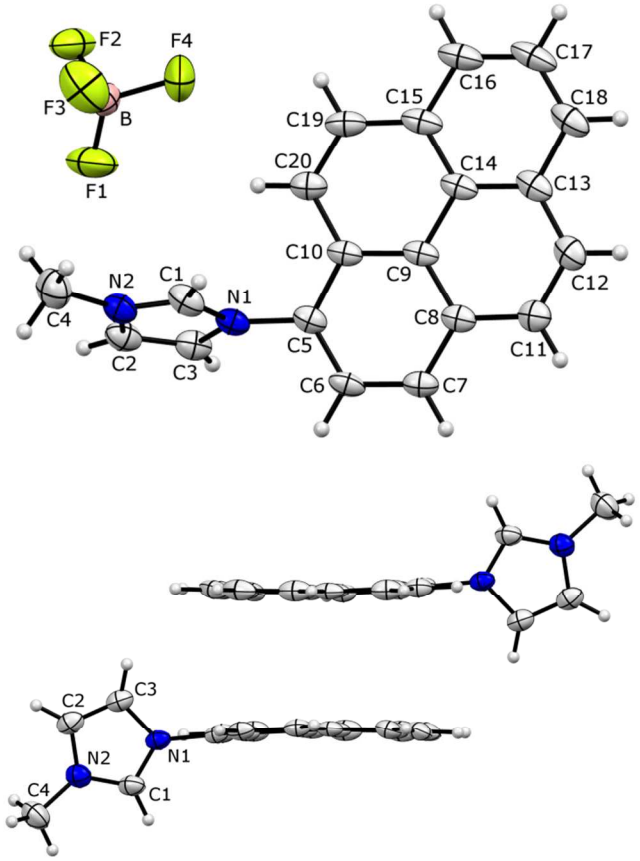

Fig. 6 Front (monomer) and side (π-dimer) Ortep views of $\mathbf{1}^{+},\mathbf{BF_4}^{-}$ crystallographic structure ($\mathbf{BF_4}^{-}$ anions are omitted for the π-dimer for clarity, plot of $\mathbf{1}^{+},\mathbf{BF_4}^{-}$ with 50% probability).

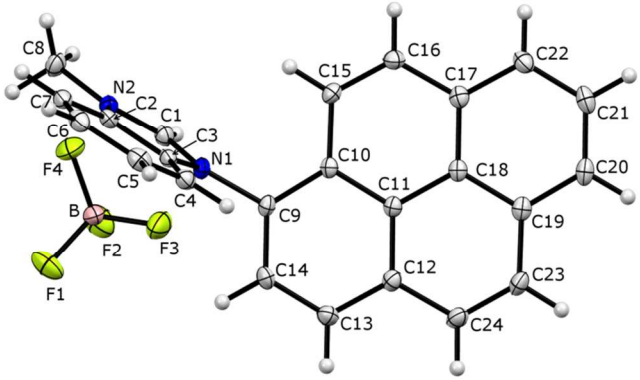

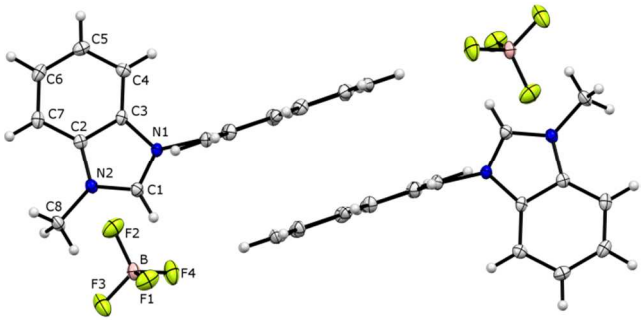

Fig. 7 Front (monomer) and side (π-dimer) Ortep views of $\mathbf{2}^{+}\mathbf{,BF_4}^{-}$ crystallographic structure (acetonitrile solvent molecules are omitted for clarity, plot of $\mathbf{2}^{+}\mathbf{,BF_4}^{-}$ with 50% probability).

stacked dimer fashion.The interplanar and the centroid to centroid (calculated from the 16 pyrene carbon atoms) distances between parallel pyrenes are equal to 3.3352(7) Å and 3.6778(7) Å, respectively, leading to a slippage distance equal to 1.5500(9) Å.

Conclusions

In summary, 1-methyl-3-(pyren-1-yl)-1*H*-imidazol-3-ium tetrafluoroborate ($\mathbf{1}^{+}\mathbf{,BF_4}^{-}$) was electrosynthesized in very good yield via a direct oxidative C-N coupling of pyrene with 1-methylimidazole, after optimization of the experimental conditions towards a more sustainable process. This reaction can be easily scaled up, can work under air, with undistilled solvent, in a one compartment cell, under galvanostatic conditions and without supporting electrolyte other than the added acid. The optimized conditions were successfully applied to the synthesis of the new 1-methyl-3-(pyren-1-yl)-1*H*-benzimidazol-3-ium tetrafluoroborate ($\mathbf{2}^{+}\mathbf{,BF_4}^{-}$), 1-methyl-4-(pyren-1-yl)-1*H*-1,2,4-triazol-4-ium tetrafluoroborate ($\mathbf{3}^{+}\mathbf{,BF_4}^{-}$) and 3-(pyren-1-yl)-benzothiazol-3-ium tetrafluoroborate ($\mathbf{4}^{+}\mathbf{,BF_4}^{-}$) compounds. These four pyren-1-yl azoliums present the characteristic procarbenic proton signal at low field and they exhibit similar UV-visible absorption spectra which are slightly bathochromically shifted as compared to the parent pyrene. Besides, whereas $\mathbf{1}^{+}\mathbf{,BF_4}^{-}$ and, to a lesser extent, $\mathbf{2}^{+}\mathbf{,BF_4}^{-}$ are highly fluorescent in solution, $\mathbf{3}^{+}\mathbf{,BF_4}^{-}$ and $\mathbf{4}^{+}\mathbf{,BF_4}^{-}$ exhibit very low emission intensity. Contrary to $\mathbf{1}^{+}\mathbf{,BF_4}^{-}$, $\mathbf{2}^{+}\mathbf{,BF_4}^{-}$and to a lesser extent $\mathbf{3}^{+}\mathbf{,BF_4}^{-}$ and $\mathbf{4}^{+}\mathbf{,BF_4}^{-}$ show an important excimer contribution. The X-ray crystallographic structures of 1-methyl-3-(pyren-1-yl)-1*H*-imidazol-3-ium tetrafluoroborate and 1-methyl-3-(pyren-1-yl)-1*H*-benzimidazol-3-ium tetrafluoroborate reveal a head-to-tail π-dimer arrangement. We wish now to exploit the very interesting pyrene physico-chemical properties to develop new organocatalysts, organometallic catalysts and multifunctional materials.

Experimental

Reagents and instrumentation

Tetraethylammonium tetrafluoroborate ($TEABF_4$) was synthesized according to the following method. Typically, in a 500 mL Erlenmeyer flask, 84.28 g of tetrafluoroboric acid, HBF_4 (Sigma Aldrich, 48% in H_2O) was mixed with 193.84 g of a solution of tetraethylammonium hydroxide, TEAOH (Alfa Aesar, 35% in H_2O). The reaction mixture was continuously stirred under air. Then, the white precipitate formed after cooling the flask in an ice bucket was isolated by filtration on a Buchner funnel. Finally, the residue was crystallized from MeOH (Carlo Erba, RPE, 99.9%) under reflux, cooled in a freezer at −18 °C, filtered on a Buchner funnel and dried at 110 °C in the stove for at least two days before use. CH_3CN (SDS, Carlo Erba, HPLC gradient 99.9%) was distilled from CaH_2 under Ar, unless otherwise noted. Et_2O (Sigma Aldrich, 99.5%, with BHT stabilizer), $HBF_4{\cdot}Et_2O$ (Sigma-Aldrich), 1-methylbenzimidazole (Alfa-Aesar, 99 %) and 1-methyl-1,2,4-triazole (Alfa-Aesar,99 %) were used as received. 1-methylimidazole (Fluka puriss, 99 %) and benzothiazole (Alfa-Aesar, 97 %) were distilled before utilization.

NMR spectra were recorded using a BRUKER 500 MHz Avance II or 300 MHz Bruker Avance III NanoBay spectrometer. ^{1}H and $^{13}C^{8}$NMR spectra were calibrated to TMS on the basis of the relative chemical shift of the solvent as an internal standard.

Mass spectra were obtained using a Bruker Micro-ToF Q instrument in ESI mode.

Elemental analyses were performed on an Analyzer CHNS/O Thermo Electron Flash EA 1112 Series.

UV/Vis absorption spectra were recorded using a Varian Cary UV/Vis spectrophotometer 50 scan using quartz cells (Hellma). In the spectroelectrochemical experiments, a UV/Vis immersion probe (Hellma, l = 2 mm) was connected through a fiber optic to the same spectrophotometer.

Emission spectra were recorded on a JASCO FP8500 spectrofluorometer in a 10 mm path-length quartz cuvette (Starna) containing 1 mL of a solution of 1.25×10^{-5} M of azolium compound in acetonitrile. Measurement parameters were common for each measured compound: λ_{ex} = 341 nm, λ_{em} = 360−600 nm, Ex and Em slits = 5 nm, 1 nm pitch, 1 s response, scan speed = 500 nm·min^{-1}, T = 20 °C.

Electrochemistry

Unless stated otherwise, all manipulations were performed using Schlenk techniques in an atmosphere of dry oxygen free argon at room temperature (T = 20 °C ± 3 °C). The supporting electrolyte (tetraethylammonium tetrafluoroborate) was degassed under vacuum before use and then dissolved to a concentration of 0.1 M. Voltammetric analyses were carried out in a standard three-electrode cell, with an Autolab PGSTAT 302 N potentiostat, connected to an interfaced computer that employed Electrochemistry Nova software. The reference electrode was a saturated calomel electrode (SCE) separated from the analyzed solution by a sintered glass disk filled with the background solution. The auxiliary electrode was a platinum wire. For all voltammetric measurements, the working electrode was a platinum electrode disk ($Ø$ = 1 mm). In these conditions, when operating in acetonitrile (0.1 M $TEABF_4$), the formal potential for the ferrocene (+/0) couple was found to be +0.40 V *vs.* SCE.

Electrolyses were performed in a cell with one or two compartments separated with glass frits of medium porosity with an Amel 552 potentiostat/galvanostat coupled with an Amel 721 electronic integrator. A platinum wire spiral (l = 50 cm, $Ø$ = 1 mm) was used as the working electrode, a platinum wire spiral (l = 50 cm, $Ø$ = 1 mm) as the counter electrode and a saturated calomel electrode as the reference electrode.

Synthesis and characterization of pyren-1-yl azoliums

General procedure for the formation of pyren-1-yl azoliums

Electrolyses were carried out under an argon atmosphere in 30 mL of acetonitrile containing 0.1 M of $TEABF_4$, pyrene (0.253 g, 1.25 mmol), nucleophile (3.75 mmol) and $HBF_4{\cdot}Et_2O$ (0.260 mL, 1.89 mmol) in a two compartment cell under vigorous stirring at room temperature (T = 20 °C ± 3 °C) and at controlled potential. Electrolyses were stopped after an uptake of 2.35-3.0 F per mol of pyrene. After evaporation of the solvent up to a volume of *ca*. 2 mL, the precipitate obtained by addition of water (100 mL) was washed with 20 mL of Et_2O and dried under vacuum.

Synthesis of 1-methyl-3-(pyren-1-yl)-1*H*-imidazol-3-ium tetrafluoroborate (1^+,BF_4^-)

Entry 2, 3, 5, Table 1

Electrolysis was performed in a two compartment cell under stirring, argon atmosphere, at room temperature, in 30 mL of acetonitrile containing 0.1 M of $TEABF_4$, pyrene (0.253 g, 1.25 mmol), 1-methylimidazole (7.53 mmol, 3.76 mmol, 2.51 mmol for entries 2, 3 and 5, respectively) and $HBF_4{\cdot}Et_2O$ (1.89 mmol for entries 2 and 3, 1.25 mmol for entry 5). The applied potential was + 1.40 V/ECS. The electrolysis was stopped after an uptake of 3.25, 2.35, 2.00 F per mol of pyrene, respectively, the solution was concentrated up to a volume of *ca*. 2 mL and 100 mL of water was added. The resulting precipitate was filtered, washed with Et_2O (20 mL) and dissolved in acetonitrile. After removing the solvent, the solid was dried under vacuum (0.425 g, 1.15 mmol, 91.8%, 0.425 g, 1.15 mmol, 91.8%, 0.345 g, 0.93 mmol, 74.5%, respectively).

Entry 4, Table 1

Electrolysis was performed in a two compartment cell under stirring, at room temperature, under an initial air atmosphere, in 30 mL of acetonitrile (HPLC grade) containing 0.1 M of $TEABF_4$, pyrene (0.253 g, 1.25 mmol), 1-methylimidazole (0.3 mL, 3.76 mmol) and $HBF_4{\cdot}Et_2O$ (0.26 mL, 1.89 mmol). The applied potential was + 1.40 V/ECS. The electrolysis was stopped after an uptake of 3.25 F per mol of pyrene, the solution was concentrated up to a volume of *ca*. 2 mL and 100 mL of water was added. The resulting precipitate was filtered, washed with Et_2O (20 mL) and dissolved in acetonitrile. After removing the solvent, the solid was dried under vacuum (0.388 g, 1.05 mmol, 83.9%).

Entry 6, Table 1

Electrolysis was performed in a two compartment cell under stirring, under Ar, at room temperature, in 165 mL of acetonitrile containing 0.1 M of $TEABF_4$, pyrene (3.500 g, 17.3 mmol), 1-methylimidazole (4.15 mL, 52.1 mmol) and $HBF_4(Et_2O)$ (3.6 mL, 26.2 mmol). The applied potential was + 1.40 V/ECS. The electrolysis was stopped after an uptake of 2.05 F per mol of pyrene, the solution was concentrated up to a volume of *ca*. 10 mL and 200 mL of water was added. The resulting precipitate was filtered, washed with Et_2O (50 mL) and dissolved in acetonitrile. After removing the solvent, the solid was dried under vacuum (6.105 g, 16.49 mmol, 95.3%).

Entry 7, Table 1

Electrolysis was performed in a one compartment cell (galvanostatic conditions, without reference electrode) under stirring, under Ar, at room temperature, in 20 mL of acetonitrile containing 0.1 M of $TEABF_4$, pyrene (4.045 g, 20.0 mmol), 1-methylimidazole (4.78 mL, 60.0 mmol) and $HBF_4{\cdot}Et_2O$ (4.12 mL, 30.0 mmol). The applied current was 50 mA. The electrolysis was stopped after an uptake of 2.05 F per mol of pyrene, the solution was concentrated up to a volume of *ca*. 10 mL and 200 mL of water was added. The resulting precipitate was filtered, washed with Et_2O (50 mL) and dissolved in acetonitrile. After removing the solvent, the solid was dried under vacuum (6.384 g, 17.25 mmol, 86.2%).

Entry 8, Table 1

Electrolysis was performed in a one compartment cell (galvanostatic conditions, without reference electrode) under stirring, under Ar, at room temperature, in 20 mL of acetonitrile containing pyrene (4.045 g, 20.0 mmol), 1-methylimidazole (4.78 mL, 60.0 mmol) and $HBF_4{\cdot}Et_2O$ (4.12 mL, 30.0 mmol). The applied current was 50 mA. The electrolysis was stopped after an uptake of 2.05 F per mol of pyrene, the solution was concentrated up to a volume of *ca*. 10 mL and 200 mL of water was added. The resulting precipitate was filtered, washed with Et_2O (50 mL) and dissolved in acetonitrile. After removing the solvent, the solid was dried under vacuum (5.930 g, 16.02 mmol, 80.1%).

1-methyl-3-(pyren-1-yl)-1*H*-imidazol-3-ium tetrafluoroborate (1^+,BF_4^-). Elemental analysis: Found: C, 64.88; H, 4.11; N, 7.61. Calc. for $C_{20}H_{15}BF_4N_2$: C, 64.90; H, 4.08; N, 7.57; λ_{max} (CH_3CN)/nm (log ε) 233 (4.62), 242 (4.76), 265 (4.36), 275 (4.58), 314 (4.01), 326 (4.36), 341 (4.51); ^{1}H NMR (DMSO-d_6, 300 MHz, 298 K) δ (ppm) 9.74 (1H, s, H2), 8.54 (1H, d, J = 8.2 Hz, H_{pyrene}), 8.50 (1H, br d, J = 2.9 Hz, H_{pyrene}), 8.47 (1H, br d, J = 3.0 Hz, H_{pyrene}), 8.42 (1H, d, J = 9.3 Hz, H_{pyrene}), 8.38 (2H, dd, J = 9.0 Hz, 7.6 Hz, H_{pyrene}), 8.30 (1H, t, J = 1.8 Hz, H4), 8.30 (1H, d, J = 8.1 Hz, H_{pyrene}), 8.23 (1H, t, J = 7.6 Hz, H_{pyrene}), 8.12 (1H, t, J = 1.7 Hz, H5), 7.92 (1H, d, J = 9.2 Hz, H_{pyrene}), 4.08 (3H, s, CH_3); ^{13}C NMR (DMSO-d_6, 75 MHz, 298 K) δ (ppm) 138.7 (C2), 132.2, 130.6, 130.1, 130.1, 129.3, 128.0, 127.3, 127.0, 126.9, 126.5, 125.7, 125.1, 124.9 (C4), 124.4, 124.2 (C5), 123.9, 123.1, 120.2, 36.3 (CH_3); HRMS (ESI-MS) m/z calcd. For $C_{20}H_{15}N_2$ $[M]^+$: 283.12298, found: 283.12195.

Synthesis of 1-methyl-3-(pyren-1-yl)-1*H*-benzimidazol-3-ium tetrafluoroborate (2^+,BF_4^-)

Entry 9, Table 1

Electrolysis was performed in a two compartment cell under stirring, under Ar, at room temperature, in 30 mL of acetonitrile containing 0.1 M of $TEABF_4$, pyrene (0.253 g, 1.25 mmol), methylimidazole (0.498 g, 3.77 mol) and $HBF_4{\cdot}Et_2O$ (0.26 mL, 1.89 mmol). The applied potential was + 1.40 V/ECS. The electrolysis was stopped after an uptake of 2.66 F per mol of pyrene, the solution was concentrated up to a volume of *ca*. 2 mL and 100 mL of water was added. The resulting white precipitate was filtered, washed with Et_2O (20 mL) and dissolved in acetonitrile. After removing the solvent, the solid was dried under vacuum (0.430 g, 1.02 mmol, 81.7%).

1-methyl-3-(pyren-1-yl)-1*H*-benzimidazol-3-ium tetrafluoroborate (2^+,BF_4^-). Elemental analysis: Found: C, 68.70; H, 4.27; N, 6.63. Calc. for $C_{24}H_{17}BF_4N_2$: C, 68.60; H, 4.08; N, 6.67; λ_{max} (CH_3CN)/nm (log ε) 234 (4.57), 242 (4.70), 265 (4.44), 276 (4.61), 315 (4.04), 327 (4.36), 342 (4.49); ^{1}H NMR (Acetone-d_6, 300 MHz, 298K) δ (ppm) 10.08 (1H, s, H2), 8.59 (1H, d, J = 8.2 Hz, H_{pyrene}), 8.51 (1H, m, H_{pyrene}), 8.48-8.36 (4H, m, H_{pyrene}), 8.31 (2H, m, H4+H_{pyrene}), 8.23 (1H, t, J = 7.7 Hz, H_{pyrene}), 7.89 (1H, m, H5), 7.83 (1H, d, J = 9.3 Hz, H_{pyrene}), 7.73 (1H, m, H6), 7.54 (1H, m, H7), 4.53 (3H, d, J = 0.5 Hz, CH_3) ;

^{13}C NMR (Acetone-d_6, 75 MHz, 298K) δ (ppm) 145.0 (C2), 134.6, 134.3, 133.4, 132.1, 131.6, 131.3, 130.7, 128.7, 128.4, 128.3, 128.2, 128.1, 127.7, 126.7, 126.5, 126.3, 125.9, 124.7, 121.3, 114.9, 114.7 (C7), 34.7 (CH_3); HRMS (ESI-MS) m/z calcd. For $C_{24}H_{17}N_2$ $[M]^+$: 333.13863, found: 333.13727.

Synthesis of 1-methyl-4-(pyren-1-yl)-1*H*-1,2,4-triazol-4-ium tetrafluoroborate (3^+,BF_4^-)

Entry 10, Table 1

Electrolysis was performed in a two compartment cell under stirring, under Ar, at room temperature, in 30 mL of acetonitrile containing 0.1 M of $TEABF_4$, pyrene (0.253 g, 1.25 mmol), 1-methyl-1,2,4-triazole (0.285 mL, 3.77 mmol) and $HBF_4{\cdot}Et_2O$ (0.260 mL, 1.89 mmol). The applied potential was + 1.40 V/ECS. The electrolysis was stopped after an uptake of 2.55 F per mol of pyrene, the solution was concentrated up to a volume of *ca*. 2 mL and 100 mL of water was added. The slightly yellow precipitate was filtered, washed with Et_2O (20 mL) and dissolved in acetonitrile. After removing the solvent, the solid was dried under vacuum (0.407 g, 1.10 mmol, 87.8%).

1-methyl-4-(pyren-1-yl)-1*H*-1,2,4-triazol-4-ium tetrafluoroborate (3^+,BF_4^-). Elemental analysis: Found: C, 61.71; H, 3.80; N, 11.18. Calc. for $C_{19}H_{14}BF_4N_3$: C, 61.49; H, 3.80; N, 11.32; λ_{max} (CH_3CN)/nm (log ε) 233 (4.58), 242 (4.73), 265 (4.34), 275 (4.55), 314 (4.00), 327 (4.34), 342 (4.49); ^{1}H NMR (DMSO-d_6, 300 MHz, 298K) δ (ppm) 10.75 (1H, s, H5), 9.79 (1H, s, H3), 8.58 (1H, d, J = 8.2 Hz, H_{pyrene}), 8.55-8.42 (4H, m, H_{pyrene}), 8.40-8.34 (2H, m, H_{pyrene}), 8.25 (1H, t, J = 7.7 Hz, H_{pyrene}), 8.07 (1H, d, J = 9.3 Hz, H_{pyrene}), 4.29 (3H, s, CH_3); ^{13}C NMR (DMSO-d_6, 75 MHz, 298K) δ (ppm) 145.5 (C3), 144.5 (C5), 132.6, 130.6, 130.3, 130.0, 129.6, 127.4, 127.1, 127.0, 126.7, 125.7, 125.1, 124.8, 124.6, 123.8, 122.9, 120.2, 39.1 (CH_3); HRMS (ESI-MS) m/z calcd. For $C_{19}H_{14}N_3$ $[M]^+$: 284.11822, found: 284.11741.

Synthesis of 3-(pyren-1-yl)-benzothiazol-3-ium tetrafluoroborate (4^+,BF_4^-)

Entry 11, Table 1

Electrolysis was performed in a two compartment cell under sonication, under Ar, shielded from light, at room temperature, in 30 mL of acetonitrile containing 0.1 M of $TEABF_4$, pyrene (0.253 g, 1.25 mmol), benzothiazole (0.41 mL, 3.75 mmol) and $HBF_4{\cdot}OEt_2$ (0.26 mL, 1.89 mmol). The applied potential was + 1.40 V/ECS. The electrolysis was stopped after an uptake of 3 F per mol of pyrene, the solution was concentrated up to a volume of *ca*. 2 mL and 100 mL of water was added. The resulting precipitate was filtered, washed with Et_2O (50 mL) and dissolved in acetonitrile. After removing the solvent, the solid was dried under vacuum (0.305 g, 0.72 mmol, 57.3%).

3-(pyren-1-yl)-benzothiazol-3-ium tetrafluoroborate (4^+,BF_4^-).

Elemental analysis: Calc. for $C_{23}H_{14}BF_4NS$: C, 65.27; H, 3.33; N, 3.31; S, 7.58; Found: C, 65.07; H, 3.37; N, 3.35; S, 7.81; λ_{max} (CH_3CN)/nm (log ε) 234 (4.65), 242 (4.79), 266 (4.39), 276 (4.51), 314 (4.12), 328 (4.32), 342 (4.38); ^{1}H NMR (Acetone-d_6, 300 MHz, 298K) δ (ppm) 11.15 (1H, s, H2), 8.81 (1H, m, H4), 8.67 (1H, d, J = 8.2 Hz, H_{pyrene}), 8.61 (1H, d, J = 8.2 Hz, H_{pyrene}), 8.57 (1H, m, H_{pyrene}), 8.53-8.42 (3H, m, H_{pyrene}), 8.33 (1H, d, J = 8.9 Hz, H_{pyrene}), 8.27 (1H, t, J = 7.6 Hz, H_{pyrene}), 8.04 (1H, m, H5), 7.92 (1H, m, H6), 7.73 (1H, m, H7), 7.71 (1H, d, J = 9.2 Hz, H_{pyrene}); ^{13}C NMR (Acetone-d_6, 125 MHz, 298K) δ (ppm) 167.5 (C7a), 143.9 (C2), 134.9, 132.6, 132.1, 131.9, 131.8 (C6), 131.6, 131.1, 130.4 (C5), 129.4, 128.6, 128.5, 128.1, 127.8, 126.6, 126.3 (C4), 125.9, 125.8, 124.6, 120.8, 118.8 (C7); HRMS (ESI-MS) m/z calcd. For $C_{23}H_{14}NS$ $[M]^+$: 336.08282, found: 336.08415.

X-ray equipment and refinement.

Diffraction data were collected on a Bruker Apex II CCD diffractometer for **1^+,BF_4^-** and on a Bruker D8 Venture Triumph Mo diffractometer for **2^+,BF_4^-** equipped with a nitrogen jet stream low-temperature system (Oxford Cryosystems) at 115 K and 100 K, respectively. The X-ray source was monochromated Mo-K_α radiation (λ = 0.71073 Å) from a sealed tube. The total number of runs and images was based on the strategy calculation from the program APEX2.[50] Semi-empirical absorption correction from equivalents was applied using SADABS.[51] Cell parameters were retrieved and refined using the SAINT software.[52] Data reduction was performed using the SAINT software[52] which corrects for Lorentz polarisation. The structure was solved by Direct Methods using the ShelXS2013[53] and refined by Least Squares using version of the ShelXL.[53] All non-hydrogen atoms were refined anisotropically. C-H hydrogen atom positions were calculated geometrically and refined using the riding model. In **1^+,BF_4^-**, three fluoride atoms were find disordered over two positions with occupation factors converged to 0.46:0.54.

Crystal structure determination of 1^+,BF_4^- and 2^+,BF_4^-.

Crystal Data for 1^+,BF_4^-. $C_{20}H_{15}BF_4N_2$ (M = 370.15 g/mol): orthorhombic, space group Pbca (no. 61), a = 11.5582(7) Å, b = 12.3717(7) Å, c = 23.8099(18) Å, V = 3404.7(4) Å^3, Z = 8, T = 115.0 K, μ(MoKα) = 0.115 mm^{-1}, *Dcalc* = 1.444 g/cm^3, 22986 reflections measured (5.914° ≤ 2Θ ≤ 54.95°), 3884 unique (R_{int} = 0.0301, R_{sigma} = 0.0249) which were used in all calculations. The final R_1 was 0.0499 (I > 2σ(I)) and wR_2 was 0.1362 (all data).

Crystal Data for 2^+,BF_4^-. $C_{26}H_{20}BF_4N_3$ (M = 461.26 g/mol): triclinic, space group P-1 (no. 2), a = 8.5758(6) Å, b = 10.4878(7) Å, c = 12.8368(8) Å, α = 75.320(2)°, β = 78.092(2)°, γ = 74.019(2)°, V = 1062.06(12) Å^3, Z = 2, T = 100.0 K, μ(MoKα) = 0.110 mm^{-1}, *Dcalc* = 1.442 g/cm^3, 52383 reflections measured (5.576° ≤ 2Θ ≤ 55.19°), 4913 unique (R_{int} = 0.0332, R_{sigma} = 0.0167) which were used in all calculations. The final R_1 was 0.0379 (I > 2σ(I)) and wR_2 was 0.1019 (all data).

Acknowledgements

The authors would like to thank the Université de Bourgogne, the Centre National de la Recherche Scientifique and the Conseil Régional de Bourgogne for their financial support. G.D.R. acknowledges a PhD support grant from the Ministère de l'Enseignement Supérieur et de la Recherche. We warmly thank Aurélien Laguerre and Dr David Monchaud for emission spectra measurements. Dr Fanny Picquet and Marie-José Penouilh are aknowledged for HR ESI-MS analyses and we thank Marcel Soustelle for elemental analyses.

Notes and references

[a] *ICMUB UMR6302, CNRS, Univ. Bourgogne Franche-Comté, F-21000 Dijon, France. Fax: +33 380396065; Tel: +33 380399125; E-mail: charles.devillers@u-bourgogne.fr; jacques.andrieu@u-bourgogne.fr*

† Electronic Supplementary Information (ESI) available: experimental details, characterization data (^{1}H and ^{13}C NMR, HRMS, elemental analyses, UV-vis absorption and emission spectroscopies), copies of ^{1}H, ^{13}C NMR and HRMS (ESI-MS) spectra for all compounds, examples of atom efficiency and E factor calculations. CCDC 1058690 (**1**$^+$,**BF**$_4^-$) and 1058691 (**2**$^+$,**BF**$_4^-$). See DOI: 10.1039/b000000x/

1. A. Laurent, *Ann. Chim. Phys.*, 1837, **66**, 136.
2. T. M. Figueira-Duarte and K. Müllen, *Chem. Rev.*, 2011, **111**, 7260.
3. R. Goedeweeck, M. Vanderauweraer and F. C. Deschryver, *J. Am. Chem. Soc.*, 1985, **107**, 2334; D. Sahoo, P. M. M. Weers, R. O. Ryan and V. Narayanaswami, *J. Mol. Biol.*, 2002, **321**, 201.
4. K. Yamana, M. Takei and H. Nakano, *Tetrahedron Lett.*, 1997, **38**, 6051; A. Laguerre, L. Stefan, M. Larrouy, D. Genest, J. Novotna, M. Pirrotta and D. Monchaud, *J. Am. Chem. Soc.*, 2014, **136**, 12406.
5. G. Venkataramana and S. Sankararaman, *Org. Lett.*, 2006, **8**, 2739.
6. J. Strauß and J. Daub, *Adv. Mater.*, 2002, **14**, 1652.
7. M. Singh, M. Holzinger, O. Biloivan and S. Cosnier, *Carbon*, 2013, **61**, 349.
8. V. Amendola, G. Bergamaschi, M. Boiocchi, L. Fabbrizzi and L. Mosca, *J. Am. Chem. Soc.*, 2013, **135**, 6345.
9. S. Karuppannan and J.-C. Chambron, *Chem. Asian J.*, 2011, **6**, 964.
10. A. A. Gorodetsky and J. K. Barton, *Langmuir*, 2006, **22**, 7917; N. Kong, J. J. Gooding and J. Liu, *J. Solid State Electrochem.*, 2014, **18**, 3379.
11. A. Le Goff, B. Reuillard and S. Cosnier, *Langmuir*, 2013, **29**, 8736.
12. S. Sabater, J. A. Mata and E. Peris, *Organometallics*, 2015, **34**, 1186.
13. F. D'Souza, R. Chitta, A. S. D. Sandanayaka, N. K. Subbaiyan, L. D'Souza, Y. Araki and O. Ito, *J. Am. Chem. Soc.*, 2007, **129**, 15865; E. W. McQueen and J. I. Goldsmith, *J. Am. Chem. Soc.*, 2009, **131**, 17554; R. Haddad, M. Holzinger, A. Maaref and S. Cosnier, *Electrochim. Acta*, 2010, **55**, 7800.
14. R. J. Waltman and J. Bargon, *J. Electroanal. Chem.*, 1985, **194**, 49; G. Zotti and G. Schiavon, *Synth. Met.*, 1992, **47**, 193.
15. L. Qu and G. Shi, *Chem. Commun.*, 2004, 2800; G. Lu, L. Qu and G. Shi, *Electrochim. Acta*, 2005, **51**, 340; Y. Gao, H. Bai and G. Shi, *J. Mater. Chem.*, 2010, **20**, 2993.
16. X. Cheng, Y. Fu, J. Zhao and Y. Zhang, *J. Appl. Polym. Sci.*, 2014, **131**, doi: 10.1002/app.39770; L. Qin, B. Lu, J. Xu, G. Zhang and S. Zhang, *RSC Advances*, 2014, **4**, 28368.
17. C.-J. Yao, J. Yao and Y.-W. Zhong, *Inorg. Chem.*, 2012, **51**, 6259; G. Feng, Z. Wang, Q. Gao, S. Chen and X. Xu, *Int. J. Electrochem. Sci.*, 2014, **9**, 5820; M. Baibarac, I. Baltog, I. Smaranda, M. Scocioreanu, J. Y. Mevellec and S. Lefrant, *Appl. Surf. Sci.*, 2014, **309**, 11.
18. N. J. Jeon, J. Lee, J. H. Noh, M. K. Nazeeruddin, M. Grätzel and S. I. Seok, *J. Am. Chem. Soc.*, 2013, **135**, 19087; K. Takemoto and M. Kimura, *RSC Advances*, 2014, **4**, 64589.
19. G. Mallesham, C. Swetha, S. Niveditha, M. E. Mohanty, N. J. Babu, A. Kumar, K. Bhanuprakash and V. J. Rao, *J. Mater. Chem. C*, 2015, **3**, 1208.
20. S. Zhang, X. Qiao, Y. Chen, Y. Wang, R. M. Edkins, Z. Liu, H. Li and Q. Fang, *Org. Lett.*, 2014, **16**, 342.
21. M. Uchimura, Y. Watanabe, F. Araoka, J. Watanabe, H. Takezoe and G.-i. Konishi, *Adv. Mater.*, 2010, **22**, 4473.
22. P. V. Vyas, A. K. Bhatt, G. Ramachandraiah and A. V. Bedekar, *Tetrahedron Lett.*, 2003, **44**, 4085; S.-W. Yang, A. Elangovan, K.-C. Hwang and T.-I. Ho, *J. Phys. Chem. B*, 2005, **109**, 16628; M. Sharif, S. Reimann, K. Wittler, L. R. Knöpke, A.-E. Surkus, C. Roth, A. Villinger, R. Ludwig and P. Langer, *Eur. J. Org. Chem.*, 2011, **2011**, 5261.
23. H. Vollmann, H. Becker, M. Corell and H. Streeck, *Justus Liebigs Ann. Chem.*, 1937, **531**, 1; G. Venkataramana and S. Sankararaman, *Eur. J. Org. Chem.*, 2005, **2005**, 4162; C.-J. Yao, L.-Z. Sui, H.-Y. Xie, W.-J. Xiao, Y.-W. Zhong and J. Yao, *Inorg. Chem.*, 2010, **49**, 8347.
24. T. M. Figueira-Duarte, S. C. Simon, M. Wagner, S. I. Drtezhinin, K. A. Zachariasse and K. Müllen, *Angew. Chem. Int. Ed.*, 2008, **47**, 10175.
25. D. N. Coventry, A. S. Batsanov, A. E. Goeta, J. A. K. Howard, T. B. Marder and R. N. Perutz, *Chem. Commun.*, 2005, 2172.
26. J. Hu, D. Zhang and F. W. Harris, *J. Org. Chem.*, 2005, **70**, 707.
27. T. Yamato, M. Fujimoto, A. Miyazawa and K. Matsuo, *J. Chem. Soc. Perkin Trans. 1*, 1997, 1201.
28. P. E. Hansen, A. Berg and H. Lund, *Acta Chem. Scand.*, 1976, **30B**, 267.
29. A. Berg, J. Lam and P. E. Hansen, *Acta Chem. Scand.*, 1986, **40B**, 665.
30. Y. Li, S. Asaoka, T. Yamagishi and T. Iyoda, *Electrochemistry*, 2004, **72**, 171.
31. T. Morofuji, A. Shimizu and J.-i. Yoshida, *J. Am. Chem. Soc.*, 2014, **136**, 4496.
32. C. H. Devillers, S. Hebié, D. Lucas, H. Cattey, S. Clément and S. Richeter, *J. Org. Chem.*, 2014, **79**, 6424.
33. M. Platon, R. Amardeil, L. Djakovitch and J.-C. Hierso, *Chem. Soc. Rev.*, 2012, **41**, 3929.
34. G. de Robillard, C. H. Devillers, D. Kunz, H. Cattey, E. Digard and J. Andrieu, *Org. Lett.*, 2013, **15**, 4410.
35. A. Tudose, L. Delaude, B. André and A. Demonceau, *Tetrahedron Lett.*, 2006, **47**, 8529.
36. A. M. Voutchkova, M. Feliz, E. Clot, O. Eisenstein and R. H. Crabtree, *J. Am. Chem. Soc.*, 2007, **129**, 12834.
37. N. Kuhn, S. M. and G. Weyers, *Naturforsch.*, 1999, **54b**, 427; M. Azouri, J. Andrieu, M. Picquet, P. Richard, B. Hanquet and I. Tkatchenko, *Eur. J. Inorg. Chem.*, 2007, **2007**, 4877; M. Azouri, J. Andrieu, M. Picquet and H. Cattey, *Inorg. Chem.*, 2009, **48**, 1236.
38. J. D. Holbrey, W. M. Reichert, I. Tkatchenko, E. Bouajila, O. Walter, I. Tommasi and R. D. Rogers, *Chem. Commun.*, 2003, 28.
39. C. H. Devillers, A. K. D. Dimé, H. Cattey and D. Lucas, *Chem. Commun.*, 2011, **47**, 1893; A. K. D. Dimé, C. H. Devillers, H. Cattey and D. Lucas, *Dalton Trans.*, 2014, **43**, 14554; S. Hebié, A. K. D. Dimé, C. H. Devillers and D. Lucas, *Chem. Eur. J.*, 2015, doi: 10.1002/chem.201404314.
40. K. Alfonsi, J. Colberg, P. J. Dunn, T. Fevig, S. Jennings, T. A. Johnson, H. P. Kleine, C. Knight, M. A. Nagy, D. A. Perry and M. Stefaniak, *Green Chem.*, 2008, **10**, 31.
41. European Chemicals Agency, http://echa.europa.eu, (accessed May 2015).
42. T. Morofuji, A. Shimizu and J.-i. Yoshida, *J. Am. Chem. Soc.*, 2013, **135**, 5000.
43. K. A. Ogawa and A. J. Boydston, *Chem. Lett.*, 2014, **43**, 907.
44. B. Trost, *Science*, 1991, **254**, 1471.
45. R. A. Sheldon, *Green Chem.*, 2007, **9**, 1273.
46. B. Bostai, Z. Novák, A. C. Bényei and A. Kotschy, *Org. Lett.*, 2007, **9**, 3437.
47. A. Kena Diba, C. Noll, M. Richter, M. T. Gieseler and M. Kalesse, *Angew. Chem. Int. Ed.*, 2010, **49**, 8367; Y. Shimakawa, T. Morikawa and S. Sakaguchi, *Tetrahedron Lett.*, 2010, **51**, 1786; S.-i. Matsuoka, Y. Ota, A. Washio, A. Katada, K. Ichioka, K. Takagi and M. Suzuki, *Org. Lett.*, 2011, **13**, 3722.
48. Y. Lin, X. Lei, Q. Yang, J. Yuan, Q. Ding, J. Xu and Y. Peng, *Synthesis*, 2012, **44**, 2699; K.-H. Chan, X. Guan, V. K.-Y. Lo and C.-M. Che, *Angew. Chem. Int. Ed.*, 2014, **53**, 2982; W.-C. Chen, Y.-C. Lai, W.-C. Shih, M.-S. Yu, G. P. A. Yap and T.-G. Ong, *Chem. Eur. J.*, 2014, **20**, 8099; S. Xu, K. Song, T. Li and B. Tan, *J. Mater. Chem. A*, 2015, **3**, 1272.
49. R. E. Taylor, P. R. Raithby and S. J. Teat, *Acta Crystallogr., Sect. E: Crystallogr. Commun.*, 2006, **62**, o1604.
50. Bruker, APEX2, version 11-0, Bruker AXS Inc., Madison, Wisconsin, USA, 2014.
51. Bruker, SADABS, version 2014/4, Bruker AXS Inc., Madison, Wisconsin, USA, 2014.
52. Bruker, SAINT, version 8.34A, Bruker AXS Inc., Madison, Wisconsin, USA, 2013.
53. G. M. Sheldrick, *Acta Crystallogr., Sect. A: Fundam. Crystallogr.*, 2008, **A64**, 112.